Chinese Chemical Letters 35 (2024) 109346

Contents lists available at ScienceDirect

Chinese Chemical Letters

journal homepage: www.elsevier.com/locate/cclet

Break of thermal equilibrium between optical and acoustic phonon branches of $CsPbI_3$ under continuous-wave light excitation and cryogenic temperature

Rongliang Deng[a,1], Yihang Chen[a,1], Xiaotong Fan[a], Guolong Chen[a], Shuli Wang[a], Changzhi Yu[a], Xiao Yang[a,c], Tingzhu Wu[a,b], Zhong Chen[a,b], Yue Lin[a,b,*]

[a] Department of Electronic Science, Fujian Engineering Research Center for Solid-State Lighting, Xiamen University, Xiamen 361005, China
[b] Innovation Laboratory for Sciences and Technologies of Energy Materials of Fujian Province (IKKEM), Xiamen 361102, China
[c] Institute of Electromagnetics and Acoustics, School of Electronic Science and Engineering, Xiamen University, Xiamen 361005, China

ARTICLE INFO

Article history:
Received 10 October 2023
Revised 13 November 2023
Accepted 27 November 2023
Available online 7 December 2023

Keywords:
$CsPbI_3$
Cs_4PbI_6
Low-temperature carrier
Lattice kinetic
Hot phonon bottleneck effect
Interfacial LO-LO interaction

ABSTRACT

The kinetic of low-temperature carrier and lattice of lead-halide perovskite is yet to be fully understood. In this work, we investigate the steady-state photoluminescences (PLs) of $CsPbI_3$ at the environmental temperature (T_e) ranging from 20 K to 300 K, and observed anomalous behaviors at cryogenic temperatures: The carrier temperature (T_c) of pure $CsPbI_3$ exhibits a negative correlation with T_e, accompanied by an expansion in Urbach tails of absorption spectra (Abs.) and excessive red-shifts at peak energy of PLs. These phenomena are also observed in those samples containing a certain amount of Cs_4PbI_6, but to a lesser extent and occurs at lower temperatures. It is attributed to the intensified hot phonon bottleneck effect (HPB) in $CsPbI_3$ at cryogenic T_e, which hinders the energy transfer from hot carriers, *via* longitudinal optics (LO) phonons to longitudinal acoustic (LA) phonons, to the ambient. For samples under continuous-wave laser excitation, in specific, the barrier induced by the enhanced HPB at low T_e prevents the effective thermalization among carriers, LO and LA phonons, which, therefore, form thermally isolated ensembles with different temperatures. At cryogenic T_e range, the elevated temperatures of carrier and LO phonon expand the high-energy side of PLs and the low-energy tail of Abs., respectively. For those samples in which the $CsPbI_3$ is mixed with Cs_4PbI_6, the interfacial LO-LO interaction across them provides a bypass for heat dissipation, mitigating the heat accumulation in LO-phonons of $CsPbI_3$. The results suggest that a strong HPB effect may break the thermal equilibrium among different branches of phonons in the lattice under certain extreme conditions.

The lead halide perovskite (LHP) $APbX_3$ ($A = Cs^+$, MA^+ and FA^+; $X = Cl^-$, Br^-, and I^-) has attracted attentions from various fields of optoelectronics [1–3]. The band-edge properties of LHP remains a hot topic with many problems remaining unclear, especially at cryogenic temperatures [4]. The band edge determines the peak photon energy of photoluminescence (PL), as well as absorption spectra (Abs.), in carrier recombination, while the interactions between carrier and lattice alter the band edge and, as a consequence, shapes of PLs and Abs. Therefore, information in PLs and Abs. are key to understanding the carrier and lattice dynamics. The processes of carrier excitation/injection and recombination includes the following steps in succession: (i) Generation of carriers; (ii) Relaxation until the Maxwell-Boltzmann distribution with a certain carrier temperature T_c is established; (iii) Scattering with lattice and cooling to band-edge; (iv) Recombination. From Stage ii to Stage iii, T_c can be significantly higher than the temperature of lattice (T_l). Therefore, the carrier at these stages is usually called “hot carrier” (HC); and the Stage iii the “HC cooling”. It has been proven that the speed of HC relaxation is highly affected by the interaction between excitons and phonons. There are two routes of electron–phonon interaction through which the energy is transferred to the lattice. At room temperature interactions between electron and lattice are dominated by Fröhlich interaction, which is the interaction between electrons and longitudinal optics (LO) phonons, while at low temperature (<30 K), it turns into interactions between electron and longitudinal acoustic (LA) phonons of deformation-potential and piezoelectric interactions [5,6]. In the transient absorption spectroscopy (TAS), a transient redistribution

* Corresponding author.
E-mail address: yue.lin@xmu.edu.cn (Y. Lin).
[1] These authors contribute equally to this work.

https://doi.org/10.1016/j.cclet.2023.109346
1001-8417/

of phonons among different states occurs right after excitation as it absorbs energy from HCs, but soon this excessive amount of energy is transferred from LO phonons to LA phonons. The energy dissipation rate in lattice depends on the density of state (DOS) of phonon, as high phonon DOS facilitates the downwards flow of energy from higher energy levels to lower ones, while the low DOS would result in hot phonons accumulation at LO branch, namely the hot phonon bottleneck (HPB) effect. The leading cause of HPB effect in $APbX_3$ is the energy gap between LO and LA phonons [7–12].

In literature, the HPB effect was commonly observed in TAS, which provides a full map of carrier kinetics with femto-second resolution, in a manner of monitoring the change in absorption of material after it being excited. It reveals a slow decrease in T_c [7]. Despite the fact that the TAS becomes a typical method of investigating the HC cooling and HPB effect, the change in absorption do not in general reflect the dynamics in radiative recombination, *i.e*., time-resolved and steady-state photoluminescences (PLs). But the luminescence property is the ultimate goal of the entire investigation and the basis on which photonics engineering is conducted. A very recent report by Lim *et al*. proposed a research on modeling the steady-state PLs of a set of iodine perovskite, from which they extract T_c and demonstrate exceptionally low thermalization coefficients in these materials [13]. In some earlier reports concerning electron–phonon interactions, steady-state PLs have been studied in theory [5,14,15], and therefore, are employed as an indicator of carrier dynamics [9,16–18]. The temperature-dependent steady-state PLs are also employed in the application of thermometry [19].

Since recently, there have been reports on optically activated A_4PbX_6 [20–22], which was later identified as possessing a sort of $APbX_3@A_4PbX_6$ core-shell structure. In this structure, the A_4PbX_6, where the PbX_6^{4+} octahedrons are detached to each other with Cs^+ ions scattered in between, encapsulates the $APbX_3$ QDs, forming a structure similar to the raisin bread ($APbX_3$: raisin, A_4PbX_6: bread) [21,22]. The $APbX_3$ QDs inside are responsible for the lumination. It was found that there exist large discrepancies in the TAS behaviors between $CsPbBr_3@Cs_4PbBr_6$ complexes and $CsPbBr_3$ QDs [11,20,23,24], which witness apparent contrasts. One group reported slower HC cooling in $CsPbBr_3@Cs_4PbBr_6$ compared with in $CsPbBr_3$ [24], whereas others reported the opposite [11,23]. However, the discrepancy actually is caused by the different excitation conditions. The former used the 310-nm laser which induces strong polaron density, while the latter two employed 400-nm excitation sources, of which the photon energy is not sufficient to excite Cs_4PbBr_6, thus no high electron–phonon interaction was induced. Despite these discrepancies, these works agreed on the fact that the contribution from LO phonons in Cs_4PbBr_6 shells and the phonon–phonon interaction across the $CsPbBr_3@Cs_4PbBr_6$ interfaces provide additional routes for the heat dissipated from HC. Therefore, comparisons between $APbX_3@A_4PbX_6$ and $APbX_3$ would provide a new aspect for studying the HBP effect.

Hitherto, one problem concerning the thermodynamics during hot carrier relaxation under steady-state excitation have been ignored. Under steady light excitation, as mentioned above, after the heat dissipating into LO phonons, the successive heat flow to the acoustic phonons is hindered by the HPB effect between LO and acoustic phonons. Is it possible that the LO phonons' temperature raises as a result of heat accumulation? If it is the case, the lattice should be separated into two sub-ensembles of LO phonons and acoustic phonons, each establishing a quasi-thermal equilibrium with different temperatures.

In this letter, we propose a research on the dynamics of carrier and lattice in temperature ranging from RT to cryogenic temperature. By analyzing the steady-state PLs on SiO_2 encapsulated $CsPbI_3$ QDs and $CsPbI_3@Cs_4PbI_6$ complex, and key parameters extracted, we observed that a strong HPB effect in $CsPbI_3$ QDs, in conjunction with high-density excitation, breaks the thermal equilibrium between LO and LA phonons of the lattice cryogenic temperature range, leading to anomalous behaviors on PLs at cryogenic temperatures. For $CsPbI_3@Cs_4PbI_6$ complex, on the contrary, the HPB effect was largely mitigated.

The samples under investigation are perovskite QDs encapsulated in all-inorganic SiO_2 particles, fabricated in a high-temperature solid-state sintering process reported in our previous work [25]. In this work, we chose two samples, the first one contains mainly $CsPbI_3$ with a trace of Cs_4PbI_6 and is denoted as S-113; the second one contains mainly Cs_4PbI_6 with a trace of $CsPbI_3$ and is denoted as S-113*. The detail of fabrication is introduced in Supporting information. The components of these two samples are demonstrated by the XRD data (Fig. S2 in Supporting information). The data collected for S-113 and S-113* are respectively dominated with characteristic peaks of $CsPbI_3$ and Cs_4PbI_6. For S-113, there is a peak of Cs_4PbI_6 observed around 12°, indicating the trace of Cs_4PbI_6. The reason that no characteristics peaks of $CsPbI_3$ is observed in the XRD of S-113* is ascribed to its low mole ratio that falls below the detection limit of XRD. In spite of that, the ~700-nm peaks in PL (Fig. S1 in Supporting information) reveal the existence of $CsPbI_3$ in S-113* and definitely in S-113. Also illustrated in Fig. S1 are the PLEs and Abs., where the fingerprint 368-nm peaks in Abs. spectra of both samples indicate the existence of Cs_4PbI_6. Here the SiO_2 shell functions as a rigid mechanical protection for the QDs inside from encroaching of water steam and oxygen. Also, the pressure exerted by the SiO_2 shell on the QDs, which estimated to fall around 0.5 GPa, prevents the degradation to yellow phase [26].

The temperature-dependent PLs of the two samples are illustrated in Fig. 1. In general, PLs of both of the samples exhibit redshift in peak energy with shrinkage in line-width as the environmental temperature (T_e) decreases. When T_e becomes lower than 60 K, two shoulder peaks emerge in the PLs of $CsPbI_3$ (Fig. S5 in Supporting information), while the PLs of Cs_4PbI_6 exhibit a single peak as the T_e goes all the way down to 20 K. The integrated PL intensities of the two samples increases with the decreasing T_e (Fig. S3 in Supporting information), although the peak intensity of S-113 decreases dramatically when multiple peaks emerge when T_e goes below 50 K (Fig. S4 in Supporting information).

We extracted the carrier temperature (T_c) by fitting the exponential high-energy tail of these PLs (Fig. S6 in Supporting information) [9]. As shown in Fig. 2a, the plots of T_c against T_e, it turns out that the T_c are much higher than T_e. As T_e decreases from 300 K, the T_c of two samples decreases initially, but after reach respective minima, both of them increase at low-T_e range, starting from 120 K and 50 K for S-113 and S-113*, respectively.

With the information of T_c, we also obtained the Abs. from PLs, according to the method introduced by Bhattacharya *et al.* [13,27]. As illustrated in Fig. S7 (Supporting information), the Abs. exhibits a slide below the band-edge, which is called the Urbach tail [18,28]. By linear fitting, we obtained the Urbach energy (E_U) from the slope of the Urbach tail. which is plotted against T_e in Fig. 2b. Note that due to the emergence of multi-peaks, the fitting of Abs. under $T_e = 50$ K may not render the correct E_U, thus they are plotted in grey. In Fig. 2b, it is evident that, in contrast to the previous literature which reported a monotonous correlation between E_U and T_e, the E_U of these two sample decrease as T_e goes down, after showing minimum at 110 K and 70 K for S-113 and S-113*, respectively, they increase as T_e continues going downwards.

According to Cody's theory [28], the Urbach tail is a revelation of lattice disorder and can be measured by the Urbach energy E_U. The lattice disorder may have multiple origins, such as Fröhlich interaction between excitons and LO phonons [6], crystalline defects [29], and halide composition [4]. The first category strongly

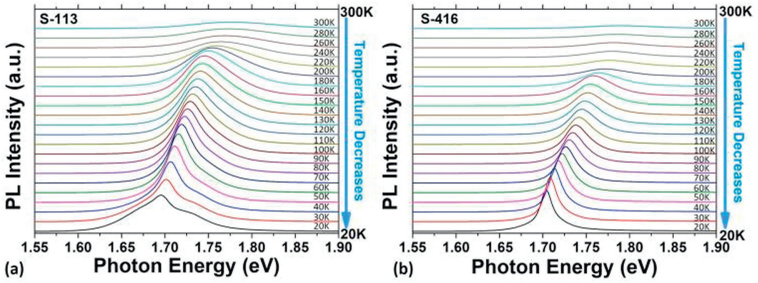

Fig. 1. Temperature-dependent PLs of (a) $CsPbI_3$ and (b) Cs_4PbI_6. The T_e at which each PL is captured is mark on the right.

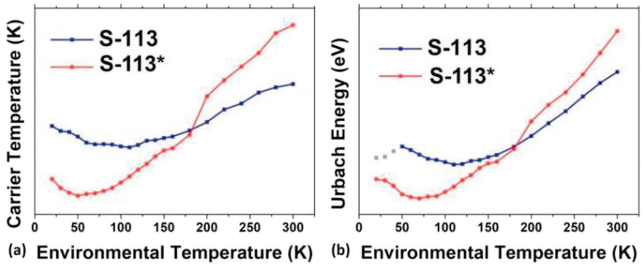

Fig. 2. (a) Carrier temperature T_c and (b) Urbach energy of both samples at different environmental temperatures.

depends on lattice temperature, which is the temperature of LO phonons (T_{LO}); the latter two are temperature independent [30]. The E_U can therefore be expressed of T_{LO}-dependent term plus T_{LO}-independent term as in Eq. 1.

$$E_U(T_{LO}, X) = \frac{\theta}{\sigma_0}\left[\frac{1+X}{2} + \frac{1}{e^{\left(\frac{A}{T_{LO}}\right)} - 1}\right] \quad (1)$$

In Eq. 1, the fitting parameters of θ and σ_0 being the Einstein temperature and steepness index, respectively; The θ denotes characteristic temperature in the Einstein model below which the thermal excitations of the phonons start to "freeze out". The σ_0 represents an order unity [28]; the X in the first term indicates the temperature-independent contribution from defects, and the second term exhibits a monotonic increase with T_{LO}, corresponding to the exciton-LO interaction. Therefore, could the anomalous increase in E_U indicate a raise in T_{LO} with decreasing T_e? It is plausible, once one gets involved the anomalous increase in T_c and the HPB effect in TAS. As mentioned previously, the HBP effect prevent the heat transfer from HC *via* LO and acoustic phonons to the ambient. Under CW excitation, HCs continuously absorb energy from the laser while transferring it to LO phonons, which should successively dissipate heat to acoustic phonons. The scarce DOS between LO branch and acoustic branch create a gap that hinders heat down-transfer. On the one hand, the HPB effect causes the storage of heat in LO phonons, raising T_{LO}, further resulting in excessively high T_c; On the other hand, as the heat flow from LO to acoustic phonon is partially blocked, the latter is cooled down by the ambient as T_e decreases and the gap between acoustic and LO branches is further enlarged.

One could also note a lesser decoupling among T_c, T_{LO} and T_e in S113*. This is due to the LO-LO interaction between $CsPbI_3$ and Cs_4PbI_6 on the interface [11]. The first-principle calculation indicates that the DOS of phonon of the heterojunction of $CsPbI_3$-Cs_4PbI_6 is far higher than that of $CsPbI_3$ (Fig. S8 in Supporting information), which greatly mitigates the HPB effect and the decoupling among T_c, T_{LO} and T_e as well. The increase in T_c and E_U cannot be a result of inefficient cooling, due to the following reasons. In Figs. 1 and 3, it is evident that the peak energy of

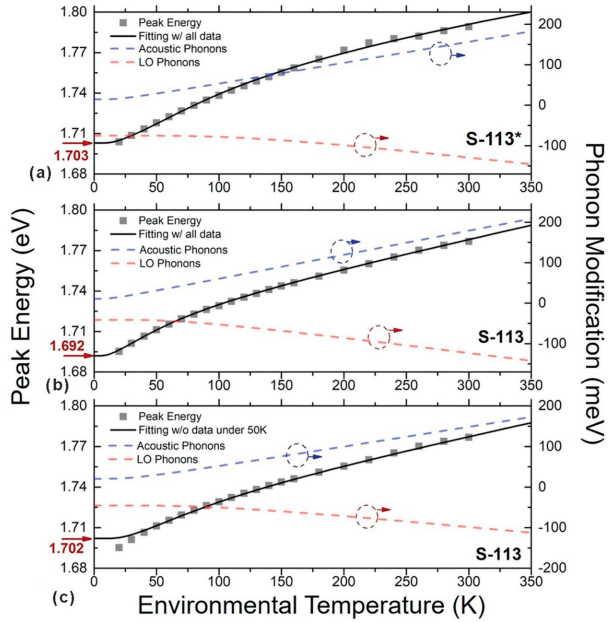

Fig. 3. Fitting of Eq. 2 on the plots of peak energy vs. T_e of S-113 and S-113*. (a) S-113* and (b) S-113 with all data involved in fitting; (c) S-113, the data captured under 50 K are excluded for fitting. The blue and dash lines illustrate the contributions of acoustic phonons and LO phonons, respectively.

PLs are monotonously decrease as T_e goes down. If under very low temperature, *e.g.*, $T_e < 50$ K, the heat fails to be conducted into the ambient, the whole temperature of the sample should be elevated since the excitation laser is continuously conveying the energy. In this case, the peak energy should increase with the deceasing T_e. The PL integral intensities of both samples, shown in Fig. S3 exhibit monotonous increase with decreasing temperature. If the heat dissipation fails at low $T_e < 50$ K, it should have decreased. Such cases were never observed in our experiment. Therefore, the heat transfer from sample to ambient is always normal.

The HBP effect in CW excitation prevents the thermalization among HCs, LO phonons and acoustic phonons, which in consequence form ensembles that are no longer in thermal equilibrium with each other. Inside each ensemble, however, thermal equilibrium is established. Therefore, these ensembles have their own temperatures, which are different from other's. As the heat dissipation from lattice to ambient *via* interaction with acoustic phonons is always efficient, the temperature of acoustic phonons could be regarded as the same with T_e. This assumption can be further verified by fitting the plot of peak energy against T_e, with a modified version of the model introduced by Göbel and Saran *et al.* [14,17] which gives the modifications on PL peak energy from exciton-LO and exciton-acoustic phonons. We change the temperatures in-

volved in this model into T_{LO} and T_e, specific ones corresponding to LO phonons and acoustic phonons, as shown in Eq. 2.

$$E_0(T) = E_0 + \frac{A_{ac}}{M_{ac}\omega_{ac}}\left(\frac{1}{e^{\frac{\hbar\omega_{ac}}{kT_e}}-1}+\frac{1}{2}\right) + \frac{A_{LO}}{M_{LO}\omega_{LO}}\left(\frac{1}{e^{\frac{\hbar\omega_{LO}}{kT_{LO}}}-1}+\frac{1}{2}\right) \quad (2)$$

The first term E_0 in Eq. 2 is the intrinsic band-gap at 0 K. The second (red dashes, Fig. 3) is the modification *via* exciton-LA coupling which expands the band-gap as T_e increases. The third term (blue dashes, Fig. 3) is exciton-LO coupling, which shrinks the band-gap, canceling the expansion induced by the second term as T_e increases. Due to the small energy of LA phonons, at elevated temperature the condition of $kT >> \hbar\omega_{ac}$ is always fulfilled. The second term is therefore reduced to linearity.

Firstly, we assume $T_e = T_{LO}$, by fitting the data of peak-energy vs. T_e of both samples by Eq. 2, we obtain curves in Fig. 3a for S-113* and Fig. 3b for S-113. Both fittings go well and the parameters are listed in Table S2 (Supporting information). However, we found that these fittings yield different peak energy E_{p0} at 0 K − 1.703 eV and 1.692 eV for S-113* and S-113, respectively. It is unreasonable as in these two samples the emitting centers are both $CsPbI_3$ QDs. Noting that the PLs of S-113 feature multi-peak at $T_e < 50$ K region, we fit the data of S-113 collected above 50 K, and yielded $E_{p0} = 1.702$ eV, which is very close to 1.703 eV of S-113*, as illustrated by the black line in Fig. 3c. We attribute this discrepancy to the intensified HPB effect at $T_e < 50$ K region, as has been mentioned previously. At this region from 50 K, the true T_{LO} is larger than T_e. This causes severer exciton-LO interaction that would narrow the bandgap, which is the reason that the peak energy data collected under 50 K are all lower than the theoretical prediction by those above 50 K. It also indicates the break of thermal equilibrium, or its origin, the HBP effect, only come into effect at $T_e <$ 50 K region for S-113. When $T_e > 50$ K, one could expect a thermal equilibrium over the whole QDs. With this model in mind, the nature of the high-energy peak in PLs under 50 K of S-113 may be the anti-Stokes replica of the main peak, as the elevated T_{LO} and T_c facilitate the phonon emission and absorption by excitons.

We note that the SiO_2 shell in the sample only serves as the protections for NCs, and do not apparently play any roles in the process of excitation and recombination. However, the anomalous expansion in Urbach tail below 50 K with decreasing T_e has not been observed in literature, where no rigid encapsulation with high pressure was applied. We therefore proposed that it is the pressure on the QDs that altered the lattice vibration which leads to the enhanced bottleneck effect. After all the pressure is so large that the NC appears in sphere shape rather than the normally cubic ones as it does when there is no confinement.

In summary, the HPB effect is intensified at cryogenic temperatures for $CsPbI_3$ QDs. Its manifestations can be observed in the steady-state PL under CW excitation as anomalous expansion in both high and low energy tails, and even the emergence of multiple peaks alongside the main one, with decreasing T_e. These are all ascribed to the temperature gradient over quasi-ensembles of carrier, LO phonons and acoustic phonons, induced by the HPB effect.

Declaration of competing interest

The authors declare that they have no known competing financial interests or personal relationships that could have appeared to influence the work reported in this paper.

Acknowledgments

This work is supported by the National Natural Science Foundation of China (Nos. 62374142, 12175189 and 11904302), External Cooperation Program of Fujian (No. 2022I0004), Fundamental Research Funds for the Central Universities (Nos. 20720190005 and 20720220085), Major Science and Technology Project of Xiamen in China (No. 3502Z20191015). The authors thank Prof. Ye Yang and Dr. Zhangqiang Yang of the College of Chemistry and Chemical Engineering at Xiamen University, for their supportive work and precious discussions.

Supplementary materials

Supplementary material associated with this article can be found, in the online version, at doi:10.1016/j.cclet.2023.109346.

References

[1] J.Y. Kim, J.W. Lee, H.S. Jung, H. Shin, N.G. Park, Chem. Rev. 120 (2020) 7867–7918.
[2] J. Yao, L. Xu, S. Wang, Z. Yang, J. Song, Nanoscale 14 (2022) 13990–14007.
[3] X. Fan, S. Wang, X. Yang, et al., Adv. Mater. 35 (2023) 2300834.
[4] M. Li, P. Huang, H. Zhong, J. Phys. Chem. Lett. 14 (2023) 1592–1603.
[5] S. Rudin, T.L. Reinecke, B. Segall, Phys. Rev. B: Condens. Matter Mater. Phys. 42 (1990) 11218–11231.
[6] J. Fu, Q. Xu, G. Han, et al., Nat. Commun. 8 (2017) 1300.
[7] Y. Yang, D.P. Ostrowski, R.M. France, et al., Nat. Photonics 10 (2015) 53–59.
[8] Z. Nie, Z. Huang, M. Zhang, et al., ACS Photonics 9 (2022) 3457–3465.
[9] H. Shi, X. Zhang, X. Sun, X. Zhang, Appl. Phys. Lett. 116 (2020) 151902.
[10] F. Sekiguchi, H. Hirori, G. Yumoto, et al., Phys. Rev. Lett. 126 (2021) 077401.
[11] Z. Nie, X. Gao, Y. Ren, et al., Nano Lett. 20 (2020) 4610–4617.
[12] J. Yang, X. Wen, H. Xia, et al., Nat. Commun. 8 (2017) 14120.
[13] J.W.M. Lim, Y. Wang, J. Fu, Q. Zhang, T.C. Sum, ACS Energy Lett. 7 (2022) 749–756.
[14] T.A. Go¨bel, M. Ruf, C.T. Cardona Lin, Phys. Rev. B 57 (1998) 15183.
[15] J. Lee, E.S. Koteles, M.O. Vassell, Phys. Rev. B: Condens. Matter Mater. Phys. 33 (1986) 5512–5516.
[16] J. Xu, S. Yu, X. Shang, X. Chen, Adv. Photonics Res. 4 (2022) 2200193.
[17] R. Saran, A. Heuer-Jungemann, A.G. Kanaras, R.J. Curry, Adv. Opt. Mater. (2017) 1700231.
[18] M. Ledinsky, T. Schonfeldova, J. Holovsky, et al., J. Phys. Chem. Lett. 10 (2019) 1368–1373.
[19] Y. Xue, Y. Chen, G. Li, et al., Chin. Chem. Lett. 35 (2024) 108447.
[20] Z. Dai, J. Chen, B. Yang, J. Phys. Chem. Lett. 12 (2021) 10093–10098.
[21] Z. Bao, C.Y. Hsiu, M.H. Fang, et al., ACS Appl. Mater. Interfaces 13 (2021) 34742–34751.
[22] M.I. Saidaminov, J. Almutlaq, S. Sarmah, et al., ACS Energy Lett. 1 (2016) 840–845.
[23] J. Zhang, C. Liu, S. Wu, et al., J. Phys. Chem. C 126 (2022) 8777–8786.
[24] G. Kaur, K.J. Babu, N. Ghorai, et al., J. Phys. Chem. Lett. 10 (2019) 5302–5311.
[25] R. Deng, X. Fan, G. Chen, et al., J. Lumin. 257 (2023) 119701.
[26] Y. Lin, X. Fan, X. Yang, et al., Small 17 (2021) 2103510.
[27] R. Bhattacharya, B. Pal, B. Bansal, Appl. Phys. Lett. 100 (2012) 222103.
[28] G.D. Cody, T. Tiedje, B. Abeles, B. Brooks, Y. Goldstein, Phys. Rev. Lett. 47 (1981) 1480–1483.
[29] C. Godet, Y. Bouizem, L. Chahed, et al., Phys. Rev. B: Condens. Matter Mater. Phys. 44 (1991) 5506–5509.
[30] M. Letz, A. Gottwald, M. Richter, L. Parthier, Phys. Rev. B 79 (2009) 195112.